OPEN ACCESS Freely available online

International Journal of Physical Medicine & Rehabilitation

Review Article

Exploration of Plant Based Inhibitors against SARS-CoV-2 Main Protease through Molecular Simulations: A Review

Divya Shaji, Ryo Suzuki, Daichi Takimoto, Yuta Hashimoto, Narutoshi Tada, Noriyuki Kurita*

Department of Computer Science and Engineering, Toyohashi University of Technology, Tempaku-cho, Toyohashi, Aichi, Japan

ABSTRACT

Coronavirus disease 2019 (COVID-19) is a pandemic first identified in China and rapidly transmitted to other countries all over the world. The lack of effective vaccines and treatments against COVID-19 causes its devastating aftermath. Therefore, it is urgently required to identify effective and safe treatments for COVID-19 and a variety of studies have been conducted for elucidating the antiviral effects of natural and plant based agents. As COVID-19 is caused by the Severe Acute Respiratory Syndrome Coronavirus 2 (SARS-CoV-2), inhibitors against SARS-CoV-2 are expected to be efficacious for the treatment of COVID-19. In this review, we will introduce the molecular simulation studies for exploring novel plant based agents as potent inhibitors against the main protease of SARS-CoV-2. These agents are expected to be utilized safely for the COVID-19 treatment.

Keywords: *In silico* drug design; Molecular simulation; Fragment molecular orbital; Molecular mechanics; Molecular dynamics; Natural product; Plant based compound; COVID-19; SARS-CoV- 2; Main protease; Inhibitor

INTRODUCTION

Coronaviruses (CoVs) are the largest group of viruses and belong to the family of *Coronaviridae*, causing respiratory and gastrointestinal infections such as the pandemic coronavirus disease 2019 (COVID-19). CoVs are categorized into four important genera that include alpha, beta, gamma, and delta. A novel member of the human CoV named "Severe Acute Respiratory Syndrome Coronavirus 2" (SARS-CoV-2) has recently emerged in China. This is a unique strain of RNA virus that has not been previously observed in humans and causes respiratory and gastrointestinal sickness in both humans and animals [1]. As there were no effective medicines or vaccines available against SARS-CoV-2, there was an urgent need for developing efficient drugs without side effects. Therefore, it was expected that plant based compounds or herbal medicines can be a rich resource for novel potent drugs against SARS-CoV-2 [2].

The application of plant based drugs has increased nowadays due to their therapeutic value, and these drugs play crucial roles in favorable health outcomes [3,4]. Before the discovery of allopathic medicines, herbal medicines were widely used for treating various types of human diseases [5]. The World Health Organization (WHO) estimates that over 80% of the world population uses plant derived medicines due to their fewer side effects and better acceptability by the human body [4]. A significant number of antiviral compounds created from various kinds of plants have been used in several studies. Researchers from all over the world have been attempting to find new natural compounds from herbal plants for preventing various diseases, including COVID-19.

SARS-CoV-2 is an enveloped beta-coronavirus with a positive strand large RNA genome belonging to the family of *Coronaviridae* [6]. The genome of SARS-CoV is similar to that of SARS- CoV-2, which has 29,891 bp and 14 Open Reading Frames (ORF) with a set of 9 sub-genomic mRNAs [7]. The 5′ end of the genome contains a single ORF that codes for 16 nonstructural proteins, which are important for viral replication and maturation, while the 3′ end of the genome contains 13 ORFs that code for structural proteins such as Envelope (E), Membrane (M), Spike (S), and Nucleocapsid (N) proteins. The creation of the viral capsid containing the viral genome and the promotion of the entrance of the virus into human cells *via* host receptors are two crucial roles served by the structural proteins of SARS-CoV-2.

Correspondence to: Noriyuki Kurita, Department of Computer Science and Engineering, Toyohashi University of Technology, Tempaku-cho, Toyohashi, Aichi, Japan, Tel: +81-532-44-6875; E-mail: kurita@cs.tut.ac.jp

Received: 08-Oct-2022, Manuscript No. JPMR-22-20582; **Editor assigned:** 10-Oct-2022, PreQC No. JPMR-22-20582 (PQ); **Reviewed:** 24-Oct-2022, QC No. JPMR-22-20582; **Revised:** 29-Dec-2022, Manuscript No. JPMR-22-20582 (R); **Published:** 06-Jan-2023, DOI: 10.35248/2329-9096.23.11.660

Citation: Shaji D, Suzuki R, Takimoto D, Hashimoto Y, Tada N, Kurita N (2023) Exploration of Plant Based Inhibitors against SARS-CoV-2 Main Protease through Molecular Simulations: A Review. Int J Phys Med Rehabil. 11:660.

The Main Protease (Mpro) of SARS-CoV-2 is a cysteine protease with a catalytic dyad (cysteine and histidine) in its active center and mediates the maturation cleavage of polyproteins during virus replication [6,8]. Mpro is a homodimer subdivided into two protomers that have three domains (Domains I, II, and III). Residues 8–101, 102–184, and 201-306 make up domains I, II, and III, respectively. Domain II is connected to domain III through a longer loop region (residues 185-200). Domains I and II contain an antiparallel barrel structure in a similar manner as the trypsin like serine proteases. Domain III is distinguished by a cluster of five α-helices. The protomers bind to each other through an N-terminal finger (residues 1-7) placed between domains II and III, which is associated with the formation of the substrate binding site in a cleft between domains I and II. As Mpro inhibits virus entry and replication, Mpro has been treated as an attractive target protein in the development of potent drugs for coronavirus infections.

Numerous computational studies have been conducted in an effort to identify natural inhibitors against SARS-CoV-2 Mpro with the purpose of developing novel drugs for the treatment of COVID-19.

LITERATURE REVIEW

In this review, we will first introduce the results of some previous *in silico* explorations of plant based inhibitors against the SARS-CoV-2 Mpro, that were based on classical Molecular Mechanics (MM) and Molecular Dynamics (MD) simulations. Next, we will introduce some results obtained by our *ab initio* molecular simulations based on molecular docking, classical MM and MD, and *ab initio* Fragment Molecular Orbital (FMO) methods. These simulated results will be useful for designing novel natural agents for the treatment of the COVID-19 pandemic.

Explorations of plant based inhibitors using MM and MD simulations

To propose natural inhibitors against SARS-CoV-2 Mpro, numerous computational studies have been conducted. Semenov, et al. [9] used a combination of modeling of NMR chemical shift analysis and molecular docking simulations to identify potential inhibitors against Mpro among a series of natural products. They found that berchemol, a natural extract from the seeds of *Centaurea cyanus*, showed the highest binding affinity with Mpro. Other natural products tested, including terrequinone A, betulinic acid, and 2,2-di(3-indolyl)-3-indolone, had higher binding affinity with Mpro than the native ligand. In another study [10], seventy-three natural compounds from *Withania somnifera* were screened as potent inhibitors against Mpro using molecular docking and classical MD simulations. Their results indicated that withacoagulin H contained in *Withania somnifera* had the highest binding free energy (−63.463 kJ/mol) with Mpro.

Patel, et al. investigated the potential of Mpro inhibitors from a compiled library of natural compounds with proven antiviral activities, using a hierarchical workflow of molecular docking, ADMET assessment, MD simulations, and binding free energy calculations [11]. The natural compounds withanosides V and VI, racemosides A and B, and shatavarin IX were found to exhibit higher binding affinity and bind strongly to the key residues of the ligand binding pocket of Mpro. The intermolecular key interactions between the Mpro residues and the natural compounds were also retained throughout the trajectory obtained by the 100 ns MD simulation. Free energy calculations prioritized withanosides V and VI as the top candidates as effective inhibitors against SARS-CoV-2 Mpro.

Benhander, et al. screened 30 compounds from *Allium roseum* L. as potent inhibitors against Mpro using molecular docking to determine their binding affinity with Mpro [12]. The three compounds, kaempferol-7-O-rutinoside, kaempferol-3-O-glucuronoside, and apigenin-7-O- glucoside, showed high binding affinities with Mpro. It was revealed that the interactions between the compounds and the conserved catalytic dyad Cys145 and His41, as well as other amino acids, were similar to those seen in the co-crystallized Mpro complex with its ligand.

In addition, Mahmud, et al. constructed a phytochemical dataset of 1154 compounds using deep literature mining that were screened for their ability to bind and inhibit the Mpro of SARS-CoV-2 [13].

In their docking analysis, the three most effective phytochemicals, cosmosiine, pelargonidin-3-O- glucoside, and cleomiscosin A, had binding energies of −8.4, −8.4, and −8.2 kcal/mol, respectively. The stabilities of the docked Mpro ligand complexes were also determined using classical MD simulations.

The *in silico* methods based on molecular docking, MD simulations, and molecular mechanics Poisson Boltzmann Surface Area (MM/PBSA) analysis were also used to investigate interactions between Mpro and eight natural eucalyptus compounds at the atomistic level [14]. The MD simulations showed that α-gurjunene has the highest binding energy of −20.37 kcal/mol, followed by aromadendrene with -18.99 kcal/mol, and finally allo-aromadendrene with −17.91 kcal/mol.

Das, et al. used a blind molecular docking approach to study the inhibitory potentials of natural anthraquinones against SARS-CoV-2 Mpro [15]. Alterporriol-Q, one of the thirteen anthraquinones studied, was found to be the most potent inhibitor against SARS-CoV-2 Mpro. In addition, MD simulation studies for the Mpro complex with alterporriol-Q suggest that alterporriol-Q does not alter the structure of Mpro to a significant extent.

In another study, 225 phytocompounds present in 28 Indian spices were screened for their inhibitory action against Mpro based on molecular docking and MD simulations [16]. Binding free energies between these phytocompounds and Mpro and PLpro (papain-like protease) were investigated. Pentaoxahexacyclo-Dotriacontanonaen-Trihydroxybenzoate derivative (PDT), rutin, dihyroxy-oxan-phenyl-chromen-4-one derivative (DOC), and luteolin-7-glucoside-4′- neohesperidoside were found to have promising inhibitory potential against SARS-CoV-2 Mpro and PLpro. In a similar manner, Gupta, et al. performed *in-silico* screening of 267 compounds present in curcuma longa against Mpro [17]. They found that two

compounds (1E,6E)-1,2,6,7-tetrahydroxy-1,7- bis(4-hydroxy-3-methoxyphenyl) hepta-1,6-diene-3,5-dione) and (4Z,6E)-1,5-dihydroxy-1,7-bis(4- hydroxyphenyl) hepta-4, 6-dien-3-one) exhibited high inhibitory potential against Mpro.

Withaferin A (wif A) and withanone (win), two natural compounds from the herb *Withania somnifera* (ashwagandha), have recently been shown to be able to covalently inhibit the viral protease Mpro [18]. To support their findings, cell culture, enzymatic, LC-MS/MS (liquid chromatography-mass spectrometry), computational, and equilibrium dialysis based experiments were conducted. According to density functional theory calculations, wif A and win can create stable adducts with thiols. These compounds significantly lowered the cytotoxicity of Mpro. The IC_{50} values for wif A and win were discovered to be 0.54 and 1.8 μM, respectively, and both were shown to irreversibly inhibit 0.5 μM Mpro. By using LC-MS/MS analysis, covalent adduct formation with wif A was found at the Mpro residues Cys145 and Cys300.

Explorations of plant based inhibitors using *ab initio* FMO calculations

Above mentioned molecular simulations based on classical MM and MD methods are efficient for investigating the binding affinities between a target protein and its ligands, and these simulations have been widely used in *in silico* drug design. However, as these classical methods are based on fixed force fields, the charge redistribution among a protein and its ligand cannot be considered. As a result, there is a possibility that the specific interactions between a protein and its ligand cannot be described precisely in the classical MM and MD simulations. In particular, if significant charge transfer is caused between a target protein and its ligand, its effect on the interactions cannot be considered in the classical methods. Accordingly, *ab initio* Molecular Orbital (MO) calculations are required to consider the charge redistribution. However, because a huge amount of computational memory and time is required to conduct conventional *ab initio* MO calculations for biological macromolecules like proteins and nucleic acids, these MO calculations are not practical.

To solve this problem, the *ab initio* FMO method was developed by Kitaura, et al. [19]. In this method, a target molecule is divided into small fragments, and the electronic states of the fragments and the pairs of fragments are evaluated in the presence of environmental electrostatic potentials from the surrounding fragments, and finally the electronic states of the entire molecule are evaluated from those of the monomers and pairs of the fragments. The FMO calculations also produce the interaction energies between the fragments, which are known as Inter-Fragment Interaction Energy (IFIE) [20]. In recent *in silico* drug designs, IFIE has been frequently used to investigate the specific interactions between the residues of the target protein and its ligands. In addition, suitable approaches were developed for analyzing the effect of thermal fluctuation of protein in a solvent [21-23]. The results evaluated using the *ab initio* FMO method were registered in a public database on the interactions between biomolecules and their ligands, which is called Fragment Molecular Orbital Database (FMODB) [24].

In our previous molecular simulations, the specific interactions between the SARS- CoV-2 Mpro and 35 natural compounds found in *Moringa oleifera*, *Aloe vera*, and *Night jasmine* were investigated using molecular docking, classical MM, and *ab initio* FMO methods. Based on the FMO results, we determined which compound binds to Mpro the most strongly and proposed several novel pharmacological lead compounds as a promising potent inhibitor against Mpro.

For example, niaziminin was found to have the highest binding affinity for Mpro among the 12 compounds from *Moringa oleifera*. We furthermore proposed some new compounds based on niaziminin and investigated their binding properties with Mpro. The FMO results revealed that the addition of a hydroxyl group to niaziminin increases its binding affinity to Mpro [25]. Our FMO calculations also revealed that feralolide from *Aloe vera* exhibited the highest binding affinity towards Mpro among the 14 compounds contained in *Aloe vera*, and some new compounds were proposed based on feralolide. The FMO results clarified that the addition of a hydroxyl group to feralolide significantly increases its binding affinity to Mpro [26]. These specific interactions between Mpro residues and various compounds obtained using FMO calculations can be used effectively to propose novel compounds as potent Mpro inhibitors. The details will be shown in the next section.

Our previous studies for proposing novel inhibitors against Mpro

Details of *ab initio* molecular simulations: The structures of the compounds from various parts of the plants including *Moringa oleifera*, *Aloe vera*, *Night jasmine,* and *Justicia adathoda* were optimized using the B3LYP/6-31G(d,p) method of the *ab initio* MO calculation program Gaussian 16 [27]. The charge distribution of each optimized structure was evaluated using the Restrained Electrostatic Potential (RESP) analysis with the HF/6-31G(d) method of Gaussian 16 [28]. The RESP charges were used as charge parameters in the MM force fields for the compounds. Notably the RESP charges were used in protein ligand docking simulations, MM optimizations of the Mpro–ligand complexes, as RESP charges can precisely describe the electrostatic interactions between the compounds and the Mpro residues.

To create candidate conformations of the compound bound to the ligand binding pocket of Mpro, we conducted the protein ligand docking simulations using AutoDock4.2.6 [29]. In the docking simulations, the size of the grid box was set to 19.5 × 19.5 × 19.5 $Å^3$, which was almost 1.5 times the size of the docked compound, and the center of the grid box was positioned at the center of the native ligand in the co-crystallized Mpro-ligand complex (PDB ID: 6LU7) [30,31]. The number of created candidate poses was 256, and the threshold distance for clustering these poses was set as 2 Å. The maximum number of energy evaluations (ga_num_evals) for each run was set as 2500000.

From the various clusters generated by AutoDock [29], we selected the three clusters with the larger number of poses, and representative structures from these clusters were used in the

subsequent MM and FMO calculations. To obtain stable structures for the Mpro compound complexes in water, the representative structures of the clusters were fully optimized in water by the classical MM method. In the MM optimizations, approximately 1800 water molecules existing within 8 Å of the complex surface were considered explicitly. The MM and MD simulation program AMBER 18 [32] was used for the MM optimizations. The AMBER FF99-SBLIN force field [33], TIP3P model [34], and general AMBER force field [35] were assigned to the Mpro residues, water molecules, and compounds, respectively. The criterion for the convergence of the structure optimization was set as 0.0001 kcal/mol/Å.

The binding properties between Mpro and the compound were investigated using the *ab initio* FMO method at an electronic level [19]. In the present FMO calculations, the MP2/6-31G (d) method [36,37] in ABINIT-MP ver6.0 [22] was employed. Each amino acid residues of Mpro, compound, and individual water molecules were assigned as a fragment in the present FMO calculations. This fragmentation allowed us to analyze the interactions between each amino acid residue of Mpro and the compound affected by solvating water molecules.

RESULTS AND DISCUSSION

Interactions between Mpro and compounds from *Moringa oleifera*

Moringa oleifera originates from India and grows in tropical and subtropical regions of the world. It belongs to the Moringaceae family and is commonly known as the "drumstick tree" or "horseradish tree". This miracle plant has anti-inflammatory, antioxidant, anticancer, and antidiabetic activities [38]. Many bioactive compounds have been found to be present in *Moringa oleifera*. Its leaves are commonly utilized as a source of numerous nutrients, including vitamins, carotenoids, polyphenols, phenolic acids, flavonoids, alkaloids, glucosinolates, isothiocyanates, tannins, and saponins. Numerous studies have been conducted to elucidate the ability of *Moringa oleifera* leaves to shield organisms and cells from oxidative DNA damage, which is linked to cancer and degenerative disorders [39]. It was also found that *Moringa oleifera* leaves are efficacious in the treatment of various diseases, ranging from diabetes and hypertension to typhoid fever and malaria [39,40]. Its fresh leaves provide high levels of vitamin E that are comparable to those in nuts [41]. As vitamin E inhibits cell proliferation in addition to acting as an antioxidant, *Moringa oleifera* leaves are expected to be efficacious [42]. In addition, the roots, bark, gum, fruit (pods), flowers, seeds, and seed oil of *Moringa oleifera* have numerous biological activities, including protection against gastric ulcers [43], antidiabetic [44], hypotensive [45], and anti-inflammatory properties [46]. It has been demonstrated that *Moringa oleifera* can enhance renal and hepatic functions and control thyroid hormone levels [47,48].

Recently, Xiong, et al. [49] proved that *Moringa* A, a novel compound derived from *Moringa oleifera* seeds, has virucidal properties against influenza A viruses (IAVs). It prevents viral replication of IAVs in host cells and protects against the cytopathic effects brought on by IAV-infected cells. When RAW264.7 (monocyte/marophage-like cells) was infected at a MOI (multiplicity of infection) of 1, the EC_{50} and EC_{90} values of *Moringa* A for IAVs were 1.27 and 5.30 μM, respectively [49]. In H1N1 (hemagglutinin type 1 and neuraminidase type 1) infected RAW264.7 cells, *Moringa* A was found to reduce the inflammatory cytokines Tumor Necrosis Factor alpha (TNF-α), Interleukin-6 (IL-6), Interleukin-1-beta (IL-1β), and Interferon-beta (IFN-β). Furthermore, it was shown that *Moringa* A reduced autophagy in infected cells and inhibited the production and nuclear transfer of the cellular protein Transcription Factor EB (TFEB), suggesting that this compound could have significant antiviral properties.

In our previous study [25], the *ab initio* FMO approach [19] was used to carefully analyze the total IFIEs between each compound and all residues of Mpro to identify which compound binds most strongly to Mpro. Among the 12 compounds from *Moringa oleifera*, niaziminin (M9) exhibited the highest total IFIE (−136.5 kcal/mol). Its magnitude was greater than those of the other compounds by at least 17.5 kcal/mol. It was also revealed that this compound had a strong attractive interaction with the negatively charged Glu166 residue of Mpro, resulting in its strong binding to Mpro. To propose potent Mpro inhibitors based on M9, we also tried to identify the component of M9 that was crucial for its strong binding to Mpro. It was discovered that the NH group and the oxygen atom connecting the two rings of M9 create the potent electrostatic interactions with the side chain and backbone of Glu166. Accordingly, these interactions were found to be the main reason for M9 having the largest total IFIE. Additionally, the Hydroxyl (OH) and carbonyl groups on the cyclohexane ring of M9 were found to form hydrogen bonds with the Asn142, Gly143, and Gln189 residues of Mpro. Therefore, it was concluded that the oxygen atom and these groups of M9 are necessary for preserving the strong binding between M9 and the Mpro residues [25].

Interactions between Mpro and compounds from *Aloe vera*

For millennia, people have used the *Aloe vera* plant for its benefits to their health, beauty, and skin care. The botanical name of *Aloe vera* is *Aloe barbadensis* miller. It is a pea-green, perennial, xerophytic, shrubby or arborescent plant that belongs to the Liliaceae family [50]. *Aloe vera* has been proven to suppress thromboxane, an inhibitor of wound healing, enhance wound healing, and decrease inflammation in both *in vitro* and *in vivo* experiments [51-53]. The *Aloe vera* gel contains magnesium lactate that can stop histamine from being produced, which prevents skin irritation and itching [54,55]. Additionally, it improves the production of cytokines and the immune system. The regenerative properties of *Aloe vera* are due to the presence of the compound glucomannan, which is rich in polysaccharides like mannose. The effect of glucomannan on fibroblast growth factor receptors enhances their activity and proliferation, which in turn boosts collagen synthesis. *Aloe vera* gel can help enhance wound healing by increasing the quantity of collagen in wounds as well as altering its chemical makeup and increasing collagen cross-linking [53,56]. In addition, mucopolysaccharides, amino acids, and zinc content of *Aloe vera*

can promote skin integrity, moisture retention, erythema reduction, and ulcer prevention [53,57].

Antiviral, antibacterial, anti-inflammatory, and anti-diabetic properties of *Aloe vera* was previously reported [58,59]. The presence of anthraquinones, flavonoids, minerals, vitamins, phenolic acids, sterols, and polysaccharides in this plant contributes to its antiviral action. Aloe-emodin is an anthraquinone found in *Aloe vera* and was shown to exhibit antiviral activity against the following viruses: influenza, pseudorabies, herpes simplex types 1 and 2, and varicella-zoster [59,60]. The extracts from *Aloe vera* leaves were found to have antiviral properties against the human cytomegalovirus *in vitro* [61]. Additionally, Rezazadeh, et al. [62] studied anti-herpes simplex virus type 1 activity of Aloe vera gel in *in vitro* cell culture. Aloin and aloe-emodin, two anthraquinones from *Aloe vera*, were recently revealed to exhibit ultrasound-mediated anti-influenza activity by Gansukh, et al. [63].

Our previous molecular simulations [26] revealed that the compound feralolide (A14) exhibited the highest total IFIE of −150.1 kcal/mol out of the 14 compounds contained in *Aloe vera*. The size of the IFIE was around 13.6 kcal/mol higher than the niaziminin (M9) from *Moringa oleifera*. We examined the IFIEs between the Mpro residues and A14 to clarify the cause of the higher binding affinity of A14 with Mpro. A14 had strong attractive interactions with Glu166 and additional Mpro residues Leu27, Asn142, and Leu167, which led to a significant overall IFIE. Therefore, it was determined that these residues were mostly responsible for the major interaction between Mpro and A14. Strong hydrogen bonds (1.51 and 1.59 Å) were formed by two hydroxyl groups at the upper end of A14 with Glu166 and the peptide backbone between Glu166 and Leu167. Additionally, the hydroxyl group of A14 created a hydrogen bond with the peptide backbone between Thr26 and Leu27, while the carbonyl group produced a hydrogen bond with the amide group of Asn142 [26].

Interactions between Mpro and compounds from *Nyctanthes arbor-tristis*

The *Night jasmine (Nyctanthes arbor-tristis)* is a small tree or shrub with flaky gray bark that can grow up to 10 meters tall. This plant is a member of the Oleaceae family and has various therapeutic uses. *Nyctanthes arbor-tristis* is widely used in traditional medicines to treat obstinate diseases such as sciatica, arthritis, and intermittent fevers. It was demonstrated that the crude extracts from the plant have pharmacological activity against inflammation, malaria, viral infection, and leishmaniasis to act as an immunostimulant [64,65]. Flavonoids, steroids, terpenes, alkaloids, and aliphatic compounds were discovered in various *Nyctanthes arbor-tristis* tissues. Alkaloids and glycosides are the two main classes of compounds produced by this plant [66]. These extracts were the subject of several investigations on their pharmacological activities, including antibacterial, anti-diabetic, antioxidant, anti-cancer, anti-allergic, anti-malarial, and antiviral effects. Arbortristosides A and C, isolated from *Nyctanthes arbor-tristis,* were found to have antiviral activity against the encephalomyocarditis virus and the Semliki Forest virus [67,68].

In previous molecular simulations [26], we selected nine compounds from the plant *Nyctanthes arbor-tristis* and investigated their specific interactions with the Mpro residues using the *ab initio* FMO method. As the compound anthocyanin (N8) had a positive charge and interacted with the Mpro residues in different manners compared with the other uncharged compounds, we excluded N8 in the investigations. The magnitudes of the total IFIEs of the eight uncharged compounds were significantly lower than those of the compounds contained in *Aloe vera* and *Moringa oleifera*. Apigenin (N9) had the highest total IFIE (−94.8 kcal/mol) of the eight *Nyctanthes arbor-tristis* compounds selected. N9 was found to interact strongly only with Glu166 *via* electrostatic interactions, indicating that Glu166 is a key residue for the strong interaction between Mpro and N9.

However, the magnitude of the total IFIE between Mpro and N9 was smaller than that of feralolide (A14) because no residue other than Glu166 of Mpro strongly interacted with N9. As a result, it was elucidated that N9 and other compounds from *Nyctanthes arbor-tristis* are not suitable for a potent Mpro inhibitor.

To elucidate the reason why N9 binds to Mpro less strongly than A14, we compared their specific interactions with the Mpro residues existing around the binding site. Three hydroxyl groups in A14 contribute significantly to forming strong hydrogen bonds with the Mpro residues, whereas only one hydroxyl group in N9 forms a hydrogen bond with Glu166. As a result, the IFIE magnitude of N9 was much smaller than that of A14. The comparison of A14 and N9 showed that the number and location of hydroxyl groups in the compounds significantly affect the specific interactions between Mpro and those compounds [26].

Interactions between Mpro and compounds from *Justicia adhatoda*

Justicia adhatoda is a popular plant medication used in Ayurvedic and Unani treatments. This plant belongs to the Acanthaceae family [69] and has been used to treat a wide range of illnesses and disorders, notably problems with the respiratory system. Accordingly, *Justicia adhatoda* is a key herb in the Ayurvedic system used to treat the symptoms of the common cold, bronchitis, and asthma [70,71]. This plant is also known as Malabar nut or Vasaka, and it tastes bitter and has an unpleasant odor [71]. *Justicia adhadoda* leaves were shown to have antiviral properties against Herpes Simplex Viruses (HSV) *in vitro* in a study by Chavan, et al. [72]. Moreover, it has antibacterial and anti-inflammatory properties. In Wistar rats, administration of *Justicia adhatoda* extracts improved neutrophils' ability to adhere to nylon fibers. Additionally, using the test specimens induced delayed type hypersensitivity responses in sheep erythrocytes, the immune modulatory function of *Justicia adhatoda* was confirmed [73,74]. Shahriar, et al. [74,75] showed that the methanolic fraction of *Justicia adhatoda* has a remarkable thrombolytic activity.

In the recent study, we selected 16 compounds from the plant *Justicia adhatoda* and investigated their binding properties with

Mpro using the same molecular simulations used for the compounds from the other plants, to propose more potent plant-based inhibitors against Mpro. Their chemical structures and properties are shown in Figure 1 and Table 1, respectively. The SwissADME webtool [76] was used to obtain the chemical characteristics of the compounds. According to Lipinski's rule of five [77], an orally active drug must meet the following criteria: (1) Molecular Weight (MW) is less than 500 g/mol, (2) Number of H-bond acceptors is less than 10, (3) Number of H-bond donors is less than 5, (4) Octano l-water partition coefficient (MLogP) is less than 5. As indicated in Table 1, all compounds from *Justicia adhatoda* meet the Lipinsky's rule. The other significant properties such as Total Polar Surface Area (TPSA) and the number of rotatable bonds were also estimated using Swiss ADME [76]. TPSA and the number of rotatable bonds for an orally active drug should be less than 140 Å^2 and 10, respectively. As listed in Table 1, all compounds satisfy the conditions.

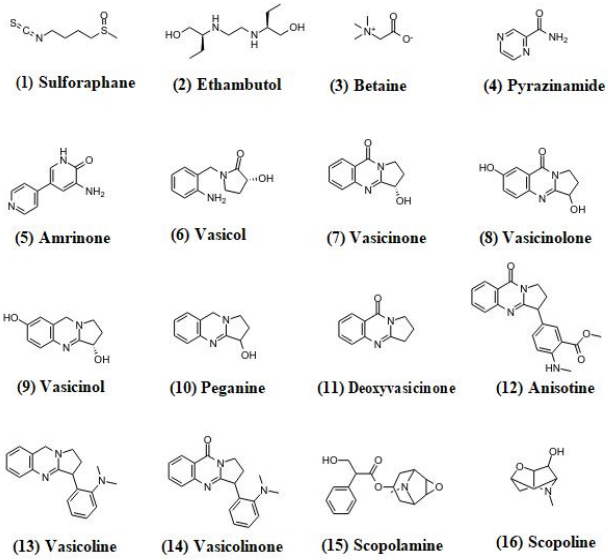

Figure 1: Chemical structures of the 16 compounds contained in *Justicia adhatoda*.

Table 1: Chemical properties of the sixteen compounds contained in *Justicia adhatoda*. Their PubChem ID, Molecular Weight (MW), number of Rotatable Bonds (RB), number of H-Bond Acceptors (HBA), number of H-Bond Donors (HBD), octanol-water partition coefficient (MLogP), and Total Polar Surface Area (TPSA), calculated by SwissADME [76].

	Compound	PubChem CID	MW (g/mol)	RB	HBA	HBD	MLogP	TPSA (Å^2)
1	Sulforaphane	5350	177.3	5	2	0	1.84	80.73
2	Ethambutol	14052	204.3	9	4	4	0.18	64.52
3	Betaine	247	117.2	2	2	0	-3.67	40.13
4	Pyrazinamide	1046	123.1	1	3	1	-1.66	68.87
5	Amrinone	3698	187.2	1	2	2	0.18	71.77
6	Vasicol	92470596	206.2	2	2	2	0.32	66.56
7	Vasicinone	442935	202.2	0	3	1	0.78	55.12
8	Vasicinolone	13970119	218.2	0	4	2	0.22	75.35
9	Vasicinol	442934	204.2	0	3	2	0.99	56.06
10	Peganine	72610	188.2	0	2	1	1.57	35.83
11	Deoxyvasicinone	68261	186.2	0	2	0	2.04	34.89
12	Anisotine	442884	349.4	4	4	4	2.45	73.22
13	Vasicoline	626005	291.4	2	1	0	3.63	18.84
14	Vasicolinone	627712	305.4	2	2	0	2.85	38.13
15	Scopolamine	3000322	303.4	5	5	1	1.19	62.3
16	Scopoline	261184	155.2	0	3	1	0.02	32.7

Therefore, we investigated their binding properties with Mpro using the FMO method. The evaluated total IFIEs between all Mpro residues and each of the compounds are listed in the last column of Table 2. Compared with the total IFIEs of the *Aloe vera* and *Moringa oleifera* compounds, the size of the total IFIEs for the *Justicia adhatoda* compounds was significantly smaller. Betaine (J3) had the largest total IFIE (−103.7 kcal/mol) among the 16 compounds from *Justicia adhatoda*, whose size was 46.4 kcal/mol smaller than that (−150.1 kcal/mol) of the best compound, feralolide (A14) from *Aloe vera*. Furthermore, the other compounds had total IFIEs with sizes less than 100 kcal/mol, although they formed at most six hydrogen bonds with the Mpro residues, as indicated in Table 2. Consequently, from the perspective of their binding strength to Mpro, the compounds from *Justicia adhatoda* are not expected to be potent inhibitors against Mpro.

Table 2: Mpro residues involved in hydrogen bond interactions with the compounds contained in *Justicia adathoda*, number of hydrogen bonds in Mpro-compound complex, and total Inter Fragment Interaction Energies (IFIEs) between the compounds and all Mpro residues.

	Compound	Residues involved in H-bonds	Number of H-bonds	Total IFIE (kcal/mol)
1	Sulforaphane	No H-bonds	0	−52.3
2	Ethambutol	Gln189	2	−59.1
3	Betaine	Asn142, Gly143, Ser144, Cys145	4	−103.7
4	Pyrazinamide	Thr24, Thr26, Ser46, Met49	4	−42.5
5	Amrinone	Thr24, Thr45, Ser46, Gly143, Cys145	6	−70.7
6	Vasicol	Leu141, Gly143, Cys145, Gln189	5	−76.6
7	Vasicinone	Gly143, Ser144, Cys145, Gln189	4	−76.0
8	Vasicinolone	Gly143, Ser144, Cys145, Glu166	4	−94.8
9	Vasicinol	Glu166	2	−95.8
10	Peganine	His164	1	−55.2
11	Deoxyvasicinone	Ser144	1	−58.2
12	Anisotine	Asn142, Ser144, Cys145	3	−85.3
13	Vasicoline	Asn142	1	−72.1
14	Vasicolinone	Asn142	1	−77.1
15	Scopolamine	Thr26, Gly143, Glu166	3	−74.8
16	Scopoline	Thr45, Ser46	2	−49.4

To reveal the key interactions between Mpro residues and J3, we investigated the IFIEs between each Mpro residue and J3. As shown in Figure 2a, the residues Leu141, Asn142, Gly143, Ser144, Cys145 and Glu166 had strong attractive IFIEs, whose sizes were greater than 10 kcal/mol. The interaction structure between these residues and J3 were shown in Figure 2b, indicating that J3 has 4 hydrogen bonds with the Asn142 side chain, and the main chains of Gly143, Ser144, and Cys145. In contrast, although Glu166 has the highest IFIE (−25.2 kcal/mol), as shown in Figure 2a, Glu166 forms no hydrogen bond with J3 and interacts electrostatically with J3. In contrast, our previous molecular simulations [26] for the compounds from *Aloe vera* revealed that feralolide (A14) has the largest total IFIE among the compounds due to its strong hydrogen bonds with Glu166. Therefore, it can be concluded that the interaction between the compound and Glu166 of Mpro significantly contributes to the binding affinity of the compound with Mpro. Glu166 was also considered as crucial residue for maintaining the shape of the Mpro active site [78].

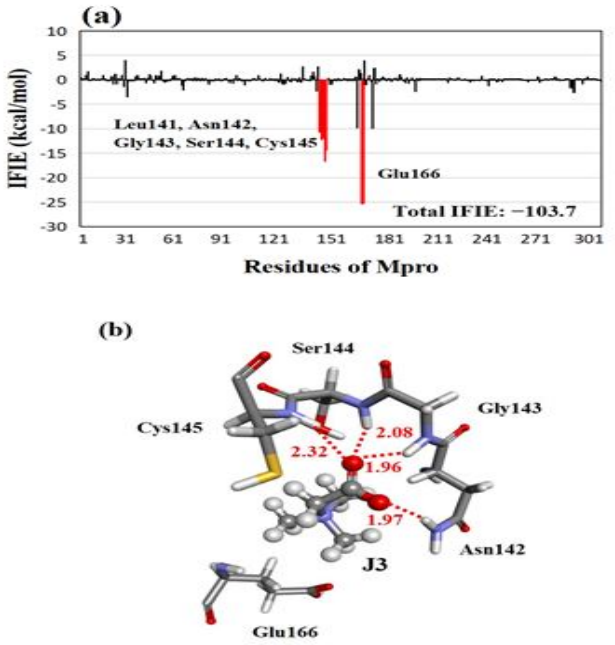

Figure 2: (a) IFIEs between the Mpro residues and the compound betaine (J3). The total IFIE of betaine (J3) with the Mpro residues is also shown. The Mpro residues with negative IFIEs whose magnitude is greater than 10 kcal/mol are indicated by red bars. (b) The interaction structure between betaine (J3) and the important Mpro residues. The hydrogen bond interactions are denoted by red lines and their distances are shown in Å.

Proposal of potent inhibitors against Mpro

To select the most suitable compound as a candidate lead agent for the Mpro inhibitor, we compared the total IFIEs of the 35 compounds contained in the above-mentioned plants. As indicated in Figure 3, anthocyanin (N8) has the largest total IFIE.

However, as N8 had a positive charge and interacted with the Mpro residues in different manners compared with the other uncharged compounds, we excluded it from the list of candidate agents. Of the other compounds, niaziminin (M9) and feralolide (A14) have rather larger total IFIEs compared with the other compounds, indicating that M9 and A14 are expected to be lead compounds for proposing novel potent inhibitors against Mpro.

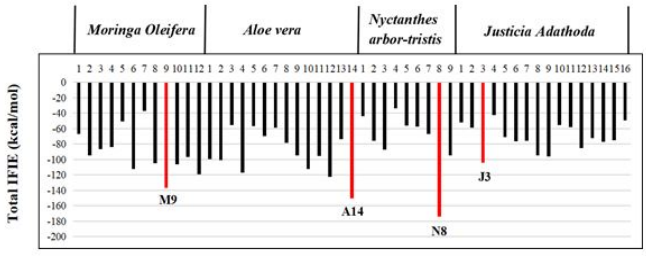

Figure 3: Total IFIEs of compounds from the plants Moringa oleifera, *Aloe vera*, *Nyctanthes arbor-tristis*, and *Justicia adhatoda* with the Mpro residues. The compounds from each plant that have the highest total IFIEs are shown by the red bars.

As niaziminin (M9) was found to bind most strongly to Mpro among the *Moringa oleifera* compounds, we first selected M9 as the starting compound for proposing novel potent inhibitors against Mpro [25]. As shown in Figure 4a, the hydroxyl groups of M9 mainly contributed to the strong interactions between M9 and Mpro residues. Therefore, we added a hydroxyl group to some of the possible sites in M9 to improve its interactions with Mpro. In fact, as shown in Figure 4c, we considered the seven sites in M9, as the other groups already contributed to the interactions with Mpro as indicated in Figures 4a and 4b. Each hydrogen atom at the red-marked sites in Figure 4c was replaced by a hydroxyl group to propose a novel M9 derivative, such as M9a, M9b, and so on, depending on the replaced site. Furthermore, using the *ab initio* FMO method, we investigated the total IFIEs between all Mpro residues and each of the proposed M9 derivatives to reveal which derivative binds most strongly to Mpro. As a result, it was revealed that the derivative M9d exhibited the largest total IFIE among the seven M9 derivatives and the addition of a hydroxyl group to M9 enhanced the total IFIE by 38.9 kcal/mol. To explain the enhancement, we compared the interaction structures between M9/M9d and some key residues of Mpro. As shown in Figure 4d, the hydroxyl group introduced into the phenyl ring of M9 formed a strong hydrogen bond with Phe140 of Mpro, resulting in the enhancement of interaction between M9d and Mpro. Therefore, it was concluded that M9d is a more potent Mpro inhibitor than the original M9 [25].

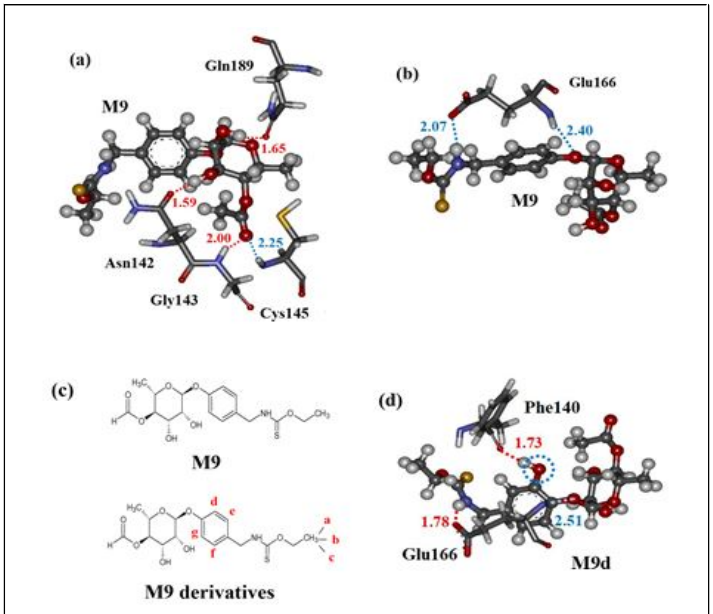

Figure 4: Interaction structure between Niaziminin (M9) contained in *Moringa oleifera* and (a) some key residues of Mpro, and (b) interaction structure between M9 and the Mpro residue Glu166. (c) Chemical structures of M9 and its derivatives, in which each hydrogen atom at the red marked sites was replaced by a hydroxyl group. (d) Interaction structure between Mpro key residues and our proposed compound M9d, in which the d-site of M9, shown by a blue dotted circle, was replaced by a hydroxyl group. The hydrogen bonding and electrostatic interactions are indicated by red and blue lines, respectively, and their distances are shown in Å.

Figure 3 also indicates that feralolide (A14) has the largest total IFIE among the plant based compounds employed in our simulations. Therefore, we proposed nine novel compounds based on A14 by introducing a hydroxyl group into different sites of A14 and investigated their binding properties with Mpro [26]. Using the *ab initio* FMO method, the total IFIEs between the proposed A14 derivatives and all Mpro residues were evaluated to propose novel inhibitors with higher binding affinities to Mpro. Depending on the position of hydroxylation, the total IFIE was significantly changed, and its size was significantly enhanced by the introduction of a hydroxyl group into A14. In fact, it was determined that the total IFIEs for the A14 derivatives (A14b, A14d, and A14i) exceeded 160 kcal/mol, which is at least 10 kcal/mol more than that of A14. It was also shown that adding a hydroxyl group to the d-site of A14 increased the IFIE between Glu166 and A14 by 30 kcal/mol (Figure 5c). As a result, among all the suggested A14 derivatives, A14d's total IFIE (−171.1 kcal/mol) had the largest magnitude. Figures 5a and 5b show a comparison of the interaction structures between A14/A14d and some important Mpro residues, showing that the hydroxyl group added at the d-site of A14d created an additional, strong hydrogen bond with the Glu166 of Mpro at 1.56 Å. As a result, it was determined that our suggested A14d derivative, which is based on feralolide (A14), could be a potent Mpro inhibitor.

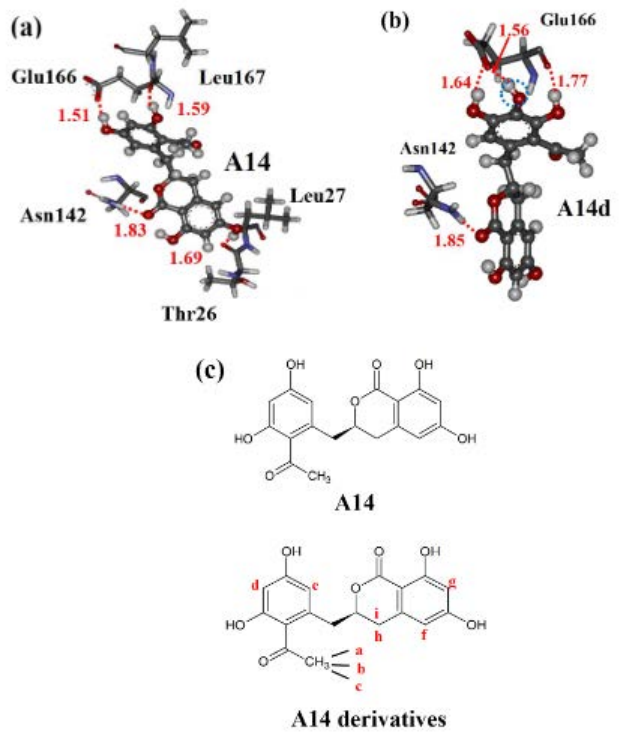

Figure 5: Interaction structures between (a) feralolide (A14) contained in Aloe vera and some key Mpro residues, and (b) A14 derivative A14d, in which the d-site of A14 shown by a blue dotted circle was replaced by a hydroxyl group, and Mpro residues. (c) Chemical structures of A14 and its derivatives, in which each hydrogen atom at the red marked sites was replaced by a hydroxyl group.

As shown in Figure 3, the total IFIEs of the compounds contained in *Nyctanthes arbor-tristis* and *Justicia adhatoda* were significantly smaller than those of the M9 and A14 compounds. Therefore, we did not consider the derivatives of these compounds in our molecular simulations.

CONCLUSION

The present COVID-19 pandemic caused by SARS-CoV-2 is a serious global health problem. Numerous molecular simulations have been carried out to identify potential lead compounds for the development of novel and safe COVID-19 treatments as well as potent inhibitors against the SARS-CoV-2 main protease. In this review, we first introduced some of the studies based on classical molecular dynamics simulations.

In addition, our recent results evaluated using the *ab initio* FMO calculations were introduced in detail. Of the selected plant-based compounds, feralolide (A14) from *Aloe vera* was found to have the highest binding affinity with the Mpro of SARS- CoV-2. Furthermore, we proposed novel compounds based on A14 and demonstrated that A14d (Figure 5c) had a higher binding affinity than the pristine A14 and that A14d could be a potent inhibitor against Mpro and a promising COVID-19 drug candidate. *In silico* drug design based on *ab initio* molecular simulations is expected to be a useful tool for predicting novel drugs for the treatment of different disorders.

ACKNOWLEDGEMENT

This work was supported by DAIKO foundation and The Hibi Science Foundation.

CONFLICTS OF INTEREST/ COMPETING INTERESTS

The authors declare no competing interests.

AVAILABILITY OF DATA AND MATERIAL

All data simulated or analyzed during this study are included in this article and the supplementary materials.

REFERENCES

1. Pal M, Berhanu G, Desalegn C, Kandi V. Severe Acute Respiratory Syndrome Coronavirus-2 (SARS-CoV-2): An Update. Cureus. 2020;12(3):e7423.
2. Soleymani S, Naghizadeh A, Karimi M. COVID-19: General strategies for herbal therapies. J Evid-Based Integr Med. 2022;27.
3. Mahmood N, Nasir SB, Hefferon K. Plant-based drugs and vaccines for COVID-19. Vaccines. 2022;9(1):15.
4. Koo Y, Song J, Bae S. Use of plant and herb derived medicine for therapeutic usage in Cardiology. Medicines. 2018;5(2):38.

5. Bhuiyan FR, Howlader S, Raihan T, Hasan M. Plants metabolites: Possibility of natural therapeutics against the COVID-19 pandemic. Front Med. 2020;7:444.
6. Mengist HM, Dilnessa T, Jin T. Structural basis of potential inhibitors targeting SARS-CoV-2 main protease. Front Chem. 2021;9:622898.
7. Kanimozhi G, Pradhapsingh B, Singh Pawar C. SARS-CoV-2: Pathogenesis, molecular targets and experimental models. Front Pharmacol. 2021;12:638334.
8. Ullrich S, Nitsche C. The SARS-CoV-2 main protease as drug target. Bioorg Med Chem Lett. 2020;30(17):127377.
9. Semenov VA, Krivdin LB. Combined computational NMR and molecular docking scrutiny of potential natural SARS-CoV-2 Mpro inhibitors. J Phys Chem B. 2022;126:2173–2187.
10. Verma S, Patel CN, Chandra M. Identification of novel inhibitors of SARS-CoV-2 main protease (Mpro) from *Withania sp.* by molecular docking and molecular dynamics simulation. J Comput Chem. 2021;42(26):1861–1872.
11. Patel CN, Jani SP, Jaiswal DG. Identification of antiviral phytochemicals as a potential SARS-CoV-2 main protease (Mpro) inhibitor using docking and molecular dynamics simulations. Sci Rep. 2021;11(1):1–3.
12. Benhander GM, Abdusalam AA. Identification of potential inhibitors of SARS-CoV-2 main protease from *Allium roseum L.* molecular docking study. Chemistry Africa. 2021;5:57–67.
13. Mahmud S, Afrose S, Biswas S, et al. Plant-derived compounds effectively inhibit the main protease of SARS-CoV-2: An *in silico* approach. PLOS ONE. 2022;17(8):e0273341.
14. Muhammad IA, Muangchoo K, Muhammad A. A computational study to identify potential inhibitors of SARS-CoV-2 main protease (Mpro) from eucalyptus active compounds. Computation. 2020;8:79.
15. Das S, Singh A, Samanta SK, Singha Roy A. Naturally occurring anthraquinones as potential inhibitors of SARS-CoV-2 main protease: An Integrated Computational Study. Biologia. 2022;77(4):1121–1134.
16. Rudrapal M, Celik I, Chinnam S, et al. Phytocompounds as potential inhibitors of SARS- CoV-2 Mpro and PLpro through computational studies. Saudi J Biol Sci. 2022;29(5):3456–3465.
17. Gupta S, Singh AK, Kushwaha PP. Identification of potential natural inhibitors of SARS-CoV2 main protease by molecular docking and Simulation Studies. J Biomol Struct Dyn. 2020;39(12):4334–4345.
18. Chakraborty S, Mallick D, Goswami M. The Natural Products Withaferin A and Withanone from the Medicinal Herb *Withania somnifera* Are Covalent Inhibitors of the SARS- CoV-2 Main Protease. J Nat Prod. 2022;85(10):2340-2350.
19. Kitaura K, Ikeo E, Asada T. Fragment molecular orbital method: An approximate computational method for large molecules. Chem Phys Lett. 1999;313(3):701–706.
20. Fedorov DG, Kitaura K. Pair Interaction Energy Decomposition Analysis. J Comput Chem. 2007;28(1):222–237.
21. Fedorov DG, Kitaura K. Energy decomposition analysis in solution based on the fragment molecular orbital method. J Phys Chem A. 2011;116:704–719.
22. Tanaka S, Mochizuki Y, Komeiji Y. Electron-correlated fragment-molecular-orbital calculations for biomolecular and Nano Systems. Phys Chem Chem Phys. 2014;16(22):10310–10344.
23. Tsukamoto T, Kato K, Kato A. Implementation of pair interaction energy DecompositionAnalysis and its applications to protein-ligand systems. J Comput Chem Jpn. 2015;14:1–9.
24. Takaya D, Watanabe C, Nagase S. FMODB: The World's first database of quantum mechanical calculations for biomacromolecules based on the fragment molecular orbital method. J Chem Inf Model. 2021;61:777–794.
25. Shaji D, Yamamoto S, Saito R. Proposal of novel natural inhibitors of severe acute respiratory syndrome coronavirus 2 main protease: Molecular docking and ab initio fragment molecular orbital calculations. Biophys Chem. 2021;275:106608.
26. Shaji D, Suzuki R, Yamamoto S. Natural inhibitors for severe acute respiratory syndrome coronavirus 2 main protease from moringa oleifera, aloe vera, and Nyctanthes arbor- tristis: Molecular docking and ab initio fragment molecular orbital calculations. Struct Chem. 2022;33:1771–1788.
27. Frisch MJ, Trucks GW, Schlegel HB. Gaussian16, Revision C.01, Gaussian, Inc., Wallingford CT. 2016.
28. Besler BH, Merz KM, Kollman PA. Atomic charges derived from semiempirical methods. J Comput Chem. 1990;11(4):431–439.
29. Morris GM, Huey R, Lindstrom W. AutoDock4 and AutoDockTools4: Automated docking with selective receptor flexibility. J Comput Chem. 2009;30(16):2785–2791.
30. Jin Z, Du X, Xu Y. Structure of Mpro from SARS-CoV-2 and discovery of its inhibitors. Nature. 2020;582:289–293.
31. Berman HM, Westbrook J, Feng Z. The Protein Data Bank. Nucleic Acids Res. 2000;28(1):235–242.
32. Case DA, Cheatham TE, Darden T. The Amber Biomolecular Simulation Programs. J Comput Chem. 2005;26:1668–1688.
33. Lindorff-Larsen K, Piana S, Palmo K. Improved side-chain torsion potentials for the Amber ff99SB protein force field. Proteins. 2010;78(8):1950–1958.
34. Jorgensen WL, Chandrasekhar J, Madura JD. Comparison of simple potential functions for simulating liquid water. J Chem Phys. 1983;79(2):926–935.
35. Wang J, Wolf RM, Caldwell JW, Kollman PA. Development and testing of a general Amber force field. J Comput Chem. 2004;25(9):1157–1174.
36. Mochizuki Y, Nakano T, Koikegami S. A parallelized integral-direct second-order Moller-Plesset perturbation theory method with a fragment molecular orbital scheme. Theor Chem Acc. 2004;112(5):442–452.
37. Mochizuki Y, Koikegami S, Nakano T. Large scale MP2 calculations with fragment molecular orbital scheme. Chem Phys Lett. 2004;396:473–479.
38. Gopalakrishnan L, Doriya K, Kumar DS. *Moringa oleifera:* A review on nutritive importance and its medicinal application. Food Sci Hum Wellness. 2016;5:49–56.
39. Vergara-Jimenez M, Almatrafi M, Fernandez M. Bioactive components in *Moringa oleifera* leaves protect against chronic disease. Antioxidants. 2017;6:91.
40. Sivasankari B, Anandharaj M, Gunasekaran P. An ethnobotanical study of indigenous knowledge on medicinal plants used by the village peoples of Thoppampatti, Dindigul District, Tamilnadu, India. J Ethnopharmacol. 2014;153(2):408–423.
41. Efiong EE, Igile GO, Mgbeje BIA. Hepatoprotective and anti-diabetic effect of combined extracts of *Moringa Oleifera* and *Vernoniaamygdalina* in streptozotocin-induced diabetic albino wistar rats. J Diabetes Endocrinol. 2013;4:45-50.
42. Borel P, Preveraud D, Desmarchelier C. Bioavailability of vitamin E in humans: An update. Nutr Rev. 2013;71(6):319–331.
43. Pal SK, Mukherjee PK, Saha BP. Studies on the antiulcer activity of *Moringa oleifera* leaf extract on gastric ulcer models in rats. Phytother Res. 1995;9:463–465.
44. Oyedepo TA, Babarinde SO, Ajayeoba TA. Evaluation of anti-hyperlipidemic effect of aqueous leaves extract of *Moringa oleifera* in alloxan induced diabetic rats. Int J Biochem Res Rev. 2013;3:162–170.

45. Faizi S, Siddiqui B, Saleem R. Hypotensive constituents from the pods of *Moringa Oleifera*. Planta Med. 1998;64(3):225–228.
46. Rao KS, Mishra SH. Anti-inflammatory and antihepatoxic activities of the roots of *Moringa pterygosperma Gaertn*. Indian J Pharm Sci. 1998;60(1):12–16.
47. Bennett RN, Mellon FA, Foidl N. Profiling glucosinolates and phenolics in vegetative and reproductive tissues of the multi-purpose trees *Moringa oleifera* L. (horseradish tree) and *Moringa stenopetala* L. J Agric Food Chem. 2003;51(12):3546–3553.
48. Tahiliani P, Kar A. Role of *Moringa oleifera* leaf extract in the regulation of thyroid hormone status in adult male and female rats. Pharmacol Res. 2001;41(3):319–323.
49. Xiong Y, Rajoka MS, Mehwish HM. Virucidal activity of moringa A from *Moringa oleifera* seeds against influenza A viruses by regulating TFEB. Int Immunopharmacol. 2021;95:107561.
50. Surjushe A, Vasani R, Saple DG. *Aloe Vera*: A short review. Indian J Dermatol. 2008;53(4):163.
51. Shelton RM. *Aloe vera*, Its chemical and therapeutic properties. Int J Dermatol. 1991;30(10):679–683.
52. Heck E, Head M, Nowak D. *Aloe vera (gel)* cream as a topical treatment for outpatient burns. Burns. 1981;7(4):291–294.
53. Hekmatpou D, Mehrabi F, Rahzani K. The effect of *Aloe vera* clinical trials on prevention and healing of skin wound: A systematic review. Iran J Med Sci. 2019;44:1.
54. Bunyapraphatsara N, Jirakulchaiwong S, Thirawarapan S, Manonukul J. The efficacy of *Aloe vera* cream in the treatment of first, second and third degree burns in mice. Phytomedicine. 1996;2(3):247–251.
55. Somboonwong J, Thanamittramanee S, Jariyapongskul A. Therapeutic effects of *Aloe vera* on cutaneous microcirculation and wound healing in second degree burn model in rats. J Med Assoc Thai. 2000;83:417–425.
56. Boudreau MD, Beland F. An evaluation of the biological and toxicological properties of *Aloe barbadensis (miller), Aloe vera*. J Environ Sci Health C Environ Carcinog Ecotoxicol Rev. 2006;24(1):103–154.
57. West DP, Zhu YF. Evaluation of *Aloe vera* gel gloves in the treatment of dry skin associated with occupational exposure. Am J Infect Control. 2003;31(1):40–42.
58. Sharrif Moghaddasi M, Res M. *Aloe vera* their chemicals composition and applications: a review. Med Chem Res. 2011;2:466–471.
59. Lowe H, Steele B, Bryant J. Antiviral activity of Jamaican medicinal plants and isolated bioactive compounds. Molecules. 2021;26(3):607.
60. Sydiskis RJ, Owen DG, Lohr JL. Inactivation of enveloped viruses by anthraquinones extracted from plants. Antimicrob Agents Chemother. 1991;35(12):2463–2466.
61. Saoo K, Miki H, Ohmori M, Winters WD. Antiviral activity of aloe extracts against cytomegalovirus. Phytother Res. 1996;10(4):348–350.
62. Rezazadeh F, Moshaverinia M, Motamedifar M, Alyaseri M. Assessment of anti-HSV-1 activity of *Aloe vera* gel extract: an *in vitro* study. J Dent. 2016;17(1):49–54.
63. Gansukh E, Gopal J, Paul D. Ultrasound mediated accelerated anti-influenza activity of *Aloe vera*. Sci Rep. 2018;8(1):17782.
64. AgrawalJ, PalA. *Nyctanthes arbor-tristis* Linn-A critical ethnopharmacological review. J Ethnopharmacol. 2013;146(3):645–658.
65. Parekh S, Soni A. *Nyctanthes arbor-tristis:* Comprehensive review on its pharmacological, antioxidant, and anticancer activities. J Appl Biol Biotech. 2020;8:95–104.
66. Jain PK, Pandey A. The wonder of Ayurvedic medicine-*Nyctanthes arbortristis*. Int J Herb Med. 2016;4(4):9–17.
67. Gupta P, Bajpai SK, Chandra K. Antiviral profile of *Nyctanthes arbortristis L.* against encephalitis causing viruses. Indian J Exp Biol. 2005;43:1156–1160.
68. Rani C, Chawla S, Mangal M. *Nyctanthes arbor-tristis* Linn. (Night Jasmine): a sacred ornamental plant with immense medicinal potentials. Ind J Tradit Knowl. 2012;11:427–435.
69. Claeson UP, Malmfors T, Wikman G. *Adhatoda vasica:* A critical review of ethnopharmacological and toxicological data. J Ethnopharmacol. 2000;72(1):1–20.
70. Karthikeyan A, Shanthi V, Nagasathya A. Preliminary Phytochemical and antibacterial screening of crude extract of the leaf of *Adhatoda vasica (L)*. Int J Green Pharm. 2009;3:78–80.
71. Sandeep D, Ramanjeet K, Seema D. A review on *Justicia adhatoda:* A potential source of natural medicine. Afr J Plant Sci. 2011;5:620–627.
72. Chavan R, Gohil DE, Shah VI. Antiviral activity of Indian medicinal plant *Justicia adhatoda* against herpes simplex virus: an in-vitro study. Int J Pharm Bio Sci. 2013;4(4):769–788.
73. Vinothapooshan G, Sundar K. Anti-ulcer activity of *Adhatoda vasica* leaves against gastric ulcer in rats. J Glob Pharma Technol. 2011;3:7–13.
74. Singh RS, Singh A, Kaur H. Promising traditional Indian medicinal plants for the management of novel Coronavirus disease: A systematic review. Phytother Res. 2021;35(8):4456–4484.
75. Shahriar M. Phytochemical screenings and thrombolytic activity of the leaf extracts of *Adhatoda vasica*. Int J Food Sci Technol. 2013;7:438–441.
76. Daina A, Michielin O, Zoete V. SwissADME: a free web tool to evaluate pharmacokinetics, drug-likeness and medicinal chemistry friendliness of small molecules. Sci Rep. 2017;7:42717.
77. Lipinski CA. Drug-like properties and the causes of poor solubility and poor permeability. J Pharmacol Toxicol Methods. 2000;44(1):235–249.
78. Juárez-Saldívar A, Lara-Ramírez EE, Reyes-Espinosa F. Ligand-based and structured-based *in silico* repurposing approaches to predict inhibitors of SARS-CoV-2 Mpro protein. Sci Pharm. 2020;88(4):54.